

5 OBSERVATIONS AND PREDICTABILITY ANALYSIS OF THE 20 APRIL 2015 XANXERE TORNADO IN SOUTHERN BRAZIL.

Maurício I. Oliveira^{1*}, Franciano S. Puhales¹, Ernani L. Nascimento¹, and Vagner Anabor¹.
¹Grupo de Modelagem Atmosférica de Santa Maria, Universidade Federal de Santa Maria, Santa Maria/RS, Brazil

1. INTRODUCTION

The southern region of Brazil, as part of the subtropical sector of South America, is one of the world's regions most favorable for tornadic activity (Brooks et al. 2003; Silva-Dias 2011; Nascimento et al 2014; among others). Although the documentation of tornado events remains poor in that region, the number of tornado reports has been increasing during the last few decades, a possible outcome of the increased access of the population to portable cameras and the Internet (Silva-Dias 2011).

During the mid-afternoon hours of 20 April 2015, the town of Xanxere, located in mid-western Santa Catarina (SC) state, southern Brazil, was struck by a (high-end) F2 tornado (Nascimento and Anabor 2015) resulting in three fatalities and ninety-seven people injured. According to official SC Civil Defense reports, over 2000 homes and buildings were total or partially destroyed, accounting for over R\$ 104 million in property damage. As the tornado tracked across the urban portions of Xanxere, it was extensively recorded in video by local residents.

The literature on tornado events in southern Brazil is scarce and, consequently, the knowledge on the atmospheric environments that favor their occurrence remains understudied. Given these points, the objective of this study is to document the synoptic- and meso-scale environments conducive to the Xanxere tornado based on the available observational datasets. To obtain a deeper understanding of the mesoscale processes that may have contributed to promoting a local ambient favorable for tornadogenesis, real data numerical simulations from the Advanced Research Weather Research and Forecast (ARW-WRF) model are performed for this tornado event. The predictability of the tornado environment is discussed in terms of a combined pattern recognition and ingredients-based analysis.

2. DATA AND METHODOLOGY

2.1. Data sources

Meteorological data used in this study include hourly measurements of 2-m air temperature, 2-m dew point temperature, 2-m relative humidity, as well as 10-m wind speed and direction and accumulated rainfall from the Automated Surface Weather Stations (ASWSs) of the Brazilian National Meteorological Institute (INMET; acronym in Portuguese) in SC and northern Rio Grande do Sul (RS). Hourly Meteorological Airport Report (METAR) from the Chapeco airport were used to support the ASWSs analysis.

Geostationary Operational Environmental Satellite 13 (GOES-13) imagery were assessed in order to identify the main mesoscale patterns prevailing around the time of the Xanxere tornadic storm. Unfortunately, the western sector of SC state is not well sampled by Doppler radars; the closest radars are located at ranges of over 200 km, and were only able to sample the upper portion of the storm. Thus, low-elevation radar signatures associated with tornadic storms, specifically supercells (e.g., hook echoes, radial velocity couplets) could not be assessed. In view of these shortcomings, still images extracted from videos of the tornado were inspected to evaluate the cloud base morphology to possible supercell characteristics of the parent storm.

Considering that no rawinsonde data exists for western SC, we evaluate the synoptic-scale setup conducive to the Xanxere tornado by relying on six-hourly analysis fields from the Climate Forecast System version 2 (CFSv2; Saha et al 2014). CFSv2 analyses have 0.5° x 0.5° latitude-longitude horizontal grid spacing and 37 vertical pressure levels. The analysis presented in this study focus on the CFSv2 analysis valid at 18:00 UTC (approximately 15:00 Local Standard Time (LST)) 20 April 2015, which is around the time when the tornado hit Xanxere. Compared with other global or regional model analyses tested, CFSv2 data were the best in representing the observed conditions in the afternoon of 20 April.

* *Corresponding author address:* Maurício I. Oliveira, Grupo de Modelagem Atmosférica de Santa Maria, Universidade Federal de Santa Maria, Santa Maria/RS, CEP.97105-900, Brazil; email: mauricio.meteorologia@gmail.com.

2.2. ARW-WRF model setup

Simulations using the ARW-WRF model version 3.6 were conducted on an Arakawa-C grid that encompassed the entire South America continent and the western [eastern] sector of the South Pacific [South Atlantic] ocean (Figure 1). The horizontal grid spacing employed in this grid was 12-km. Two higher spatial resolution (3-km and 1-km) grids were two-way nested within the 12-km grid in order to explicitly simulate the convective storms; however, the analysis of the simulation at such finer grids has not been fully investigated and is still underway. Those results will be addressed in a later study. Therefore, in this paper, we focus on the results of the 12-km grid in order to assess the mesoscale environment of the Xanxere tornadic storm.

The initial conditions utilized in this study were provided by the 00:00 UTC 20 April 2015 CFSv2 analysis fields. Lateral and boundary conditions were provided by subsequent CFSv2 analyses at 06:00, 12:00 and 18:00 UTC of 20 April. Although the simulation was run for the 24 hour period of 20 April, the model fields shown in this study are focused on the simulation valid at 18:00 UTC (the time of tornado occurrence).

The convective parameterization scheme employed in the 12-km grid is the Kain-Fritsch scheme (Kain 2004). The Mellor-Yamada-Janjic scheme (Janjic 2004) for planetary boundary layer (PBL) flow was used. The microphysics configuration chosen was the WRF Single-Moment 3-class scheme (WSM3; Hong et al 2004). The configuration of the 3-km and 1-km grids was the same as that of the 12-km grid, except that convective processes were explicitly resolved in the finer grids (i. e., the convective parameterizations were turned off).

3. RESULTS

3.1. The tornado and its parent circulation.

Figure 2 shows a sequence of still images extracted from a video of the Xanxere tornado as it crossed the northern portion of the town at around 15:00 LST. Dense rain curtains are first seen obscuring the approaching tornado from west-northwest (Figure 2a). Less than 2 minutes later, the tornado, now barely visible as it is wrapped in rain and lofted debris, damages homes and business buildings along its track across northern Xanxere (Figure 2b). After 40 seconds, the tornado moves eastwards, away from the observer, at the when time additional rain shafts hit the observer (from south-southeast) and wrap around the tornado (Figure 2c). Such rain curtains and their accompanying strong winds encircle the

tornado in a manner that is consistent with a rear flank downdraft (RFD; Lemon and Doswell, 1979; Markowski 2002). At this time in the video (not shown), the parent low-level mesocyclone is seen, as rotating cloud tags above and around the tornadic circulation.

The presence of the aforementioned features (i. e., a RFD and the tornado's parent low-level mesocyclone) indicates that the Xanxere tornado was spawned by a supercell thunderstorm. Moreover, the isolated/discrete character of the storm as seen by visible channel GOES-13 images (to be shown later) further supports the idea of the supercellular convective storm mode.

3.2. Satellite and ASWS observations

During the night hours of 20 April 2015, a Mesoscale Convective System (MCS) formed at the nose of an intense Low-Level Jet Stream (LLJS) near the Argentina-Paraguay border and northeastern Argentina (not shown). This MCS moved eastward toward southern Brazil, reaching the northwestern sector of RS still during the dawn hours of 20 April. Although the MCS was weak and decaying slowly, it maintained its eastward-northeastward movement and covered much of western SC with its extensive cloud shield (Figure 3a).

The cloud deck of the decaying MCS prevented temperature from rising significantly in western SC, as measured by the ASWS in Xanxere (not shown). The maximum hourly-measured 2-m temperature reached 23.5 °C just prior to tornado occurrence; dew point temperatures had been rising slowly throughout the day reaching approximately 21 °C. The surface temperature and moisture conditions contributed to high relative humidity values that oscillated between 82 % and 97 % during the afternoon (not shown). High PBL relative humidity values favor low lifting condensation level (LCL) heights, which in turn prevent RFD parcels from becoming too negatively buoyant and allow them to be vertically stretched in developing/intensifying vertical vortices; thus such thermodynamic conditions support the development of tornadic supercells (Markowski and Richardson 2010).

To the north of the cloud shield of the old MCS, a rapidly evolving cumulus field, seen as NW-SE-oriented cloud streets, developed in western SC, Parana state and Paraguay. Cloud streets usually are the visual manifestation of horizontal convective roll (HCR) circulations in sheared mixed layers (Markowski and Richardson 2010).

At the intersection of the leading edge of the remnants of the MCS and the HCRs, a line of discrete storms initiated, the southernmost of them becoming the Xanxere supercell (Figure 3b). One could speculate that the interaction between the cold pool of the MCS and the HCRs could be responsible for initiating the storms in western SC; furthermore, it is also possible that the vertical circulations associated with the HCRs alone could solely be responsible for triggering the convective cells. As no close-range radar observations exist for the region under study as well as dense mesoscale surface observations, understanding the convective initiation mechanisms of the Xanxere supercell and its evolution will require a thorough evaluation of the ARW-WRF high resolution simulations in future studies.

3.3. Synoptic-scale environment from CFSv2 data.

The synoptic-scale environment prevailing during the Xanxere tornado event is assessed based on CFSv2 analyses valid at 18:00 UTC 20 April 2015. At 250-hPa (Figure 4a), two merging jet streaks were located over much of the La Plata basin; western SC was situated under the anticyclone flank of the northernmost upper-level jet, under wind speeds in the 20-30 m s⁻¹ range.

The flow at the 500-hPa level was predominantly westerly, with wind speeds in the 15-20 m s⁻¹ range (Figure 4b). No apparent short wave perturbations were apparent over SC at 500-hPa, including in water vapor imagery loops from GOES-13 (not shown). In fact, the nearest short wave trough was located just west of the Andes mountain range, too far upstream of southern Brazil. Therefore, quasi-geostrophic forcing for ascent via differential vorticity advection did not seem to have played any significant role in promoting an environment favorable for tornadic storms.

A moderate intensity NW-SE-oriented LLJS advected warm, moist air from the Amazon basin into the La Plata basin (Figure 4c), contributing for creating a conditionally unstable atmosphere (Salio et al 2007). Furthermore, the LLJS also enhanced the vertical wind shear in the lower troposphere (to be discussed in the next section), an important ingredient for tornadoes (Rasmussen and Blanchard 1998; Craven and Brooks 2004; Nascimento et al 2014; Markowski and Richardson 2010).

At the surface (Figure 4d), a weak low-pressure system that extended from Paraguay to extreme northeastern Argentina and western SC maintained a horizontal mean sea level pressure

(MSLP) gradient on its eastern side, where the LLJS was immersed. This surface pressure pattern that favored the advection of warm, moist air into the warm sector was also confirmed by the MSLP and 10-m wind measurements from the ASWSs in western SC (not shown).

3.4. ARW-WRF 18 hr simulation: the mesoscale environment.

An ingredients-based analysis (Brooks et al 2003) using the 12-km ARW-WRF 18-hr simulation, valid at 18:00 UTC 20 April 2015, is performed to assess the magnitude and spatial distribution of the convective parameters commonly employed in supercell tornado forecasting (Rasmussen and Blanchard 1998; Craven and Brooks 2004).

A warm, moist air mass extended from Paraguay into the western region of SC and resulted in relatively high values of Convective Available Potential Energy for surface parcels (~1500 J kg⁻¹; Figure 5a). A west-east CAPE gradient across SC is apparent in the Figure 5a, a result of cloudiness from the previous MCS persisting in eastern SC. However, the ARW-WRF simulation overestimated surface temperatures in western SC, mainly because it underestimated the persistence as well as the thickness of the cloud deck in that region. Thus, the actual CAPE values were probably lower than in the simulation.

Another consequence of the unrealistically high surface temperature in the ARW-WRF simulation is reflected in the LCL height field (Figure 5b). The simulation produces LCL heights slightly lower than 1250 m near Xanxere which are not consistent with the low surface dew-point depressions observed in ASWS measurements in and near Xanxere in the afternoon (approximately 3 °C; not shown). The high relative humidity in the PBL, as observed by the ASWSs, was possibly associated with LCLs heights much lower.

In the middle troposphere, 700-500-hPa mean-layer lapse rate values were generally lower than 6 K km⁻¹ in western SC (Figure 5c). The low values of lapse rate suggest that the moderate CAPE values, although overestimated in the simulation, were mostly due to the warm and moist PBL. As in the Xanxere environment, Nascimento et al (2014) also did not find high values of mid-level lapse rates in their study of a tornadic supercell in southeastern Brazil.

Deep layer (0-6 km) vertical wind shear was not particularly strong over the entire SC state; values near Xanxere were slightly below 20 m s⁻¹, (Figure 5d) approximating the minimum threshold typically regarded as favorable for tornadic

supercells in severe storm environments in the United States (Markowski and Richardson 2010). Low-level shear magnitudes were compatible with supercell environments, although not particularly strong in the simulation. Storm relative helicity values in the 0-3 km [0-1 km] layer neared $-150 \text{ m}^2 \text{ s}^{-2}$ [$-50 \text{ m}^2 \text{ s}^{-2}$] (see Figures 5e and 5f, respectively). The existence of sufficient SRH in the simulation is attributed to the presence of the NW-SW LLJS that encompassed the western portion of SC.

Finally, CFSv2 data indicate a small-scale low-geopotential height area in northern RS at the 850-hPa level associated with a local intensification of the LLJS just to the north of it (not shown). Saulo et al (2007) showed that when MCSs persist for several hours, the latent heat release in their wake may induce low-level height (pressure) falls and instigate a stronger LLJS locally. However, the preliminary ARW-WRF simulations conducted in this study thus far were not able to reproduce this feature at 12-km grid spacing (the only pressure perturbations observed in the simulation were positive, mostly associated with cold pools from the simulated storms). More numerical simulations with different model configurations will be conducted to test whether the localized low-geopotential height feature is generated by latent heat release caused by the previous MCS or an artifact of the CFSv2 analysis.

4. SUMMARY AND FINAL REMARKS

The 20 April 2015 Xanxere tornadic supercell formed in a rather weakly forced large-scale environment, with no apparent short wave impulses influencing the development of the storms. Moderate winds in the upper troposphere contributed to DLS values marginally favorable for tornadic storm formation. One important ingredient for the occurrence of the Xanxere storm was the presence of an 850-hPa NW-SE-oriented LLJS that was responsible for advecting warm, moist air from the Amazon basin into western SC. The presence of lower-tropospheric heat and moisture produced an unstable atmosphere in SC which, coupled to the low-level shear associated with the LLJS, and the weak, but sufficient DLS was capable of instigating tornadic supercell development.

The presence of a cloud deck from an earlier MCS helped holding low values of dew-point temperature depressions across western SC, and therefore, low LCL heights, a necessary ingredient for tornadic supercells.

In light of the weak (or absent) dynamic forcing for ascent and the sub-optimal DLS, the

low-level kinematic and thermodynamic conditions represented in CFSv2 and AWR-WRF simulations probably were dominant in generating the supercell characteristics of the Xanxere storm. Moreover, the mesoscale complexities introduced by the pre-existing MCS make the Xanxere event a low-predictability severe weather episode when compared with other events in Brazil (Nascimento et al 2014).

Many questions were raised from this study regarding possible roles played by the previous MCS on the development of subsequent severe storms in the afternoon. Given the lack of high-resolution meteorological observations in western SC, a better understanding of such processes as well as those associated with the development of low-level rotation in the Xanxere storm depends on high-resolution numerical simulations with different parameterizations. These will be the focus of future studies on the Xanxere tornadic storm.

5. REFERENCES

- Brooks, H. E., J. W. Lee, and J. P. Craven, 2003: The spatial distribution of severe thunderstorm and tornado environments from global reanalysis data. *Atmos. Research*, **67-68**, 73-94.
- Hong, S. Y., Dudhia, J., Chen, S. H., 2004: A Revised Approach to Ice microphysics Processes for the Bulk Parameterization of Clouds and Precipitation. *Mon. Wea. Rev.*, **132**, 103-120.
- Janjic, Z. I., 1994: The Step-Mountain Eta Coordinate Model: Further Developments of the Convection, Viscous Sublayer, and Turbulence Closure Schemes. *Mon. Wea. Rev.*, **122**, 927-945.
- Kain J. S., 2004: The Kain-Fritsch Convective Parameterization: An Update. *J. Appl. Meteor.*, **43**, 170-181.
- Lemon, L. R., and Doswell, C. A., 1979: Severe Thunderstorm Evolution and Mesocyclone Structure as Related to Tornadogenesis., *Mon. Wea. Rev.*, **107**, 1184-1197.
- Markowski, P. M., 2002: Hook Echoes and Rear-Flank Downdrafts: A Review. *Mon. Wea. Rev.*, **130**, 852-876.
- _____, and Richardson, Y., 2010: Mesoscale Meteorology in Midlatitudes. John Wiley & Sons.

Nascimento, E. L., Anabor, V., 2015: Evaluation of the Intensity of the Tornado Occurred in the Town of Xanxere/SC on 20 April 2015. Tech. Note, 13p.

_____, Held, G., and A. M. Gomes, 2014: A multiple-vortex tornado in Southeastern Brazil. *Mon. Wea. Rev.*, **142**, 3017-3037.

Rasmussen, E. N., and Blanchard, D. O., 1998: Baseline climatology of sounding-derived supercell and tornado forecast parameters. *Wea. Forecasting*, **13**, 1148-1164.

Saha, S., and co-authors, 2014: The NCEP Climate Forecast System Version 2. *J. Climate.*, **27**, 2185-2208.

Salio, P., Nicolini, M., and Zipser, E., 2007: Mesoscale Convective Systems over Southeastern South America and Their Relationship with the South American Low-Level Jet. *Mon. Wea. Rev.*, **135**, 1290-1309.

Saulo, C., Ruiz, J., and Skabar, Y. G., 2007: Synergism between the Low-Level Jet and Organized Convection at Its Exit Region. *Mon. Wea. Rev.*, **135**, 1310-1326.

Silva-Dias, M. A. F., 2011: An Increase in the Number of tornado Reports in Brazil. *Wea. Soc. Clim.*, **3**, 209-217.

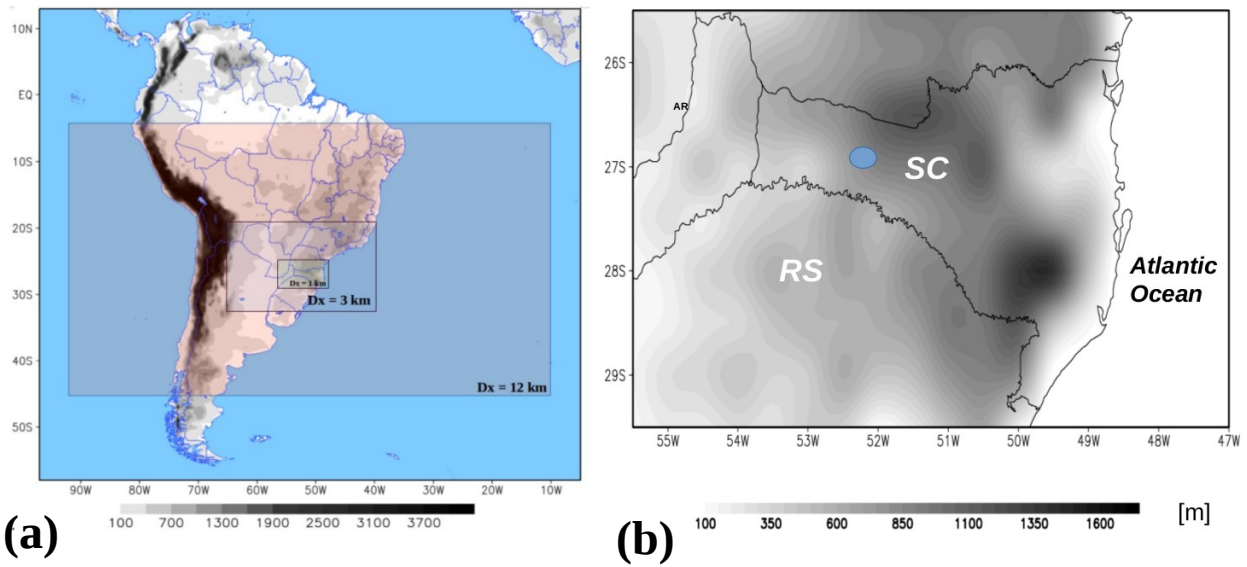
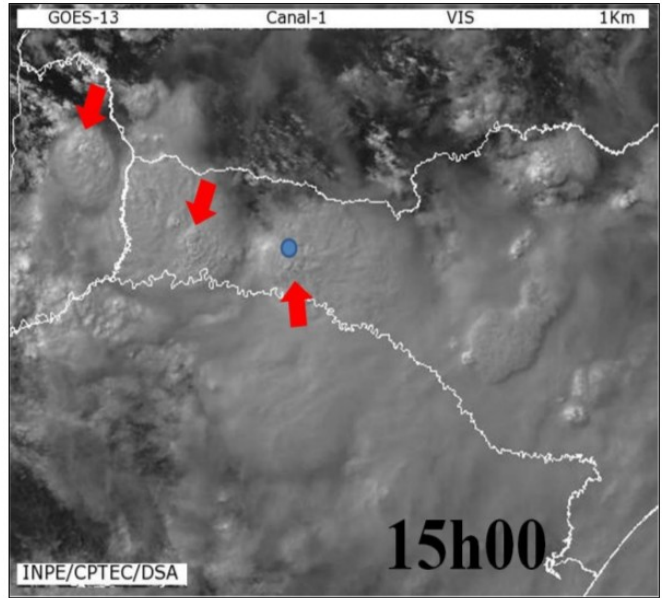
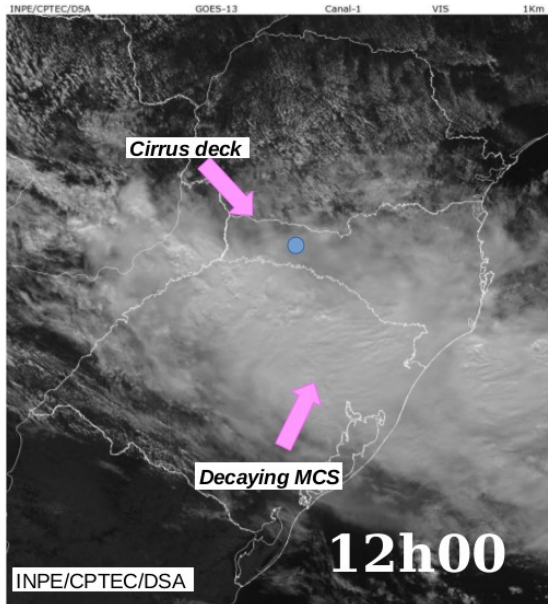


Figure 1: (a) ARW-WRF domains for the South American continent (horizontal grid spacing (Dx) = 12 km), the Southeastern sector of South America (Dx = 3 km) and the SC state (Dx = 1 km). (b) A zoomed-in view of Southern Brazil, centered on the SC state. The blue dot is the Xanxere location.



Figure 2: (a)-(c): Still images extracted from a video of the Xanxere tornado as it tracked across the northern sector of the town at approximately 18:00 UTC (15:00 h LST). (Tornado images are courtesy of Elias Collet.)

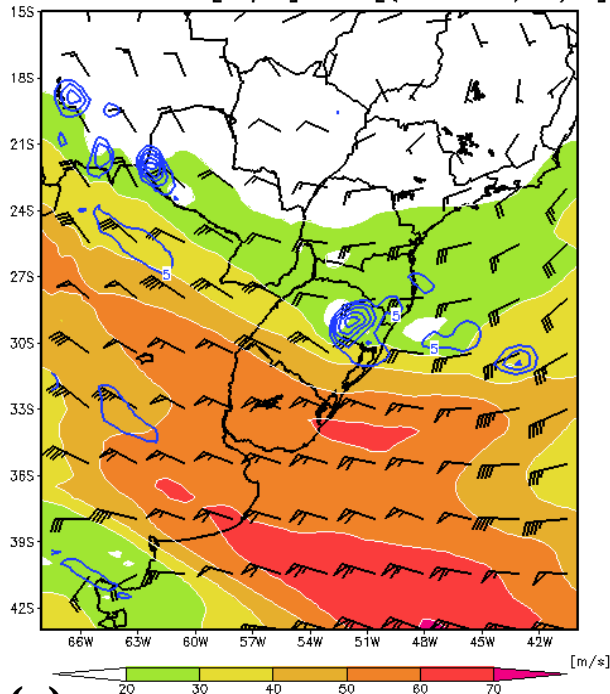


(a)

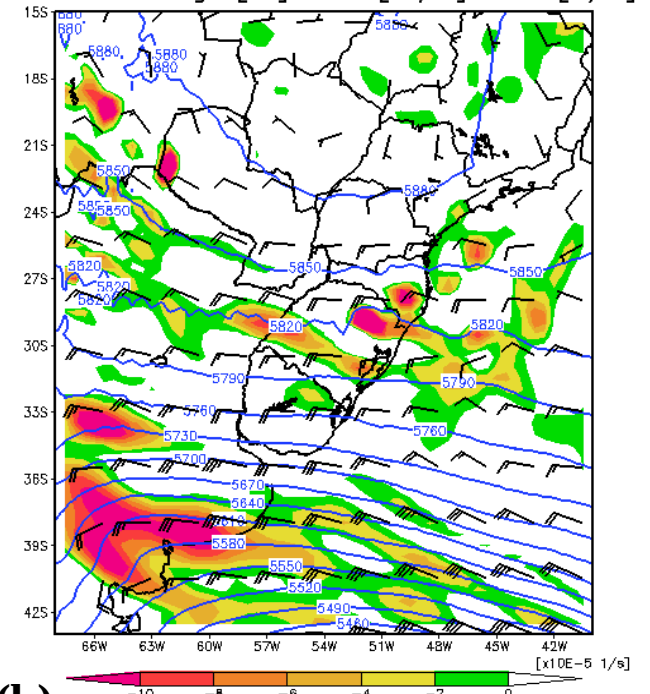
(b)

Figure 3: GOES-13 1-km resolution visible images at (a) 15:00 UTC (12:00 h LST) 20 April 2015 and (b) 18:00 UTC (15:00 h LST). Pink arrows in (a) indicate a cirrus cloud deck over western SC and the decaying MCS to in northern RS. Red arrows in (b) indicate storms developing in western SC and northeastern Argentina. The blue dot in both figures denotes the location of Xanxere.

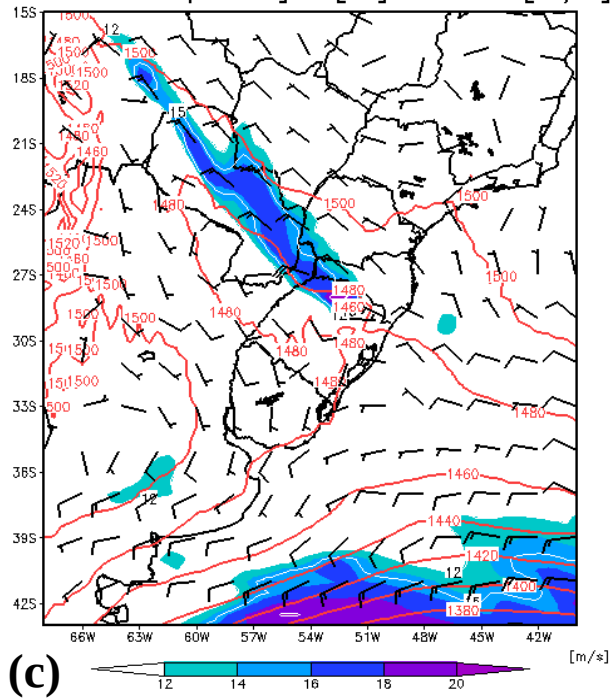
250hPa: Wind[m/s]-Div.[(x10E-5) 1/s]



500hPa: Height[m]-Wind[m/s]-Vort.[1/s]



(a) 850hPa Geop. Height [m] & wind [m/s]



(b) MSLP[hPa]-2m Temp.[C]-10m wind[m/s]

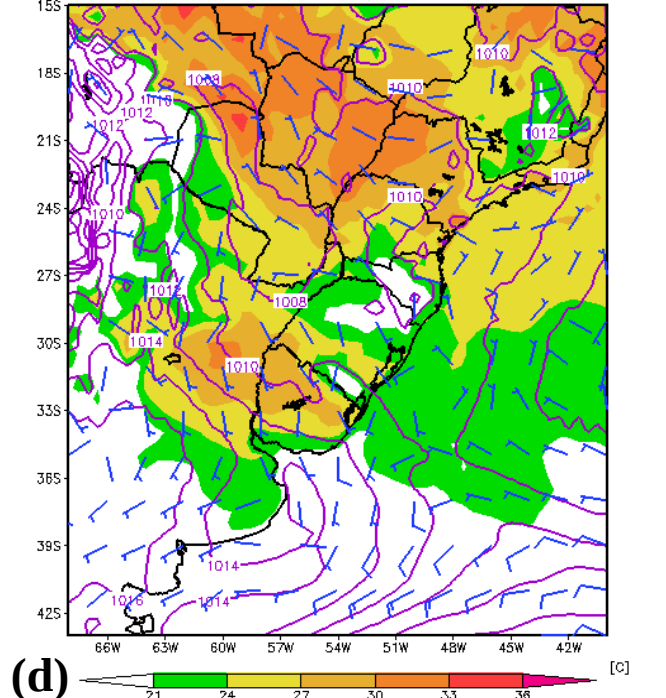


Figure 4: CFSv2 fields valid at 18:00 UTC 20 April 2015. (a) 250-hPa winds (half-barb, 5 m s⁻¹; full barb, 10 m s⁻¹, pennants; 50 ms); (b) 500-hPa wind (barbs), geopotential height (contoured at 30 gpm intervals) and relative vorticity (x10⁻⁵ s⁻¹; only negative values are shaded); (c) 850-hPa wind (barbs; shaded values above 12 m s⁻¹) and geopotential height (contoured at 20 gpm intervals). (d) 10-m wind (barbs), MSLP (contoured at 2-hPa intervals) and 2-m temperature (°C; shaded).

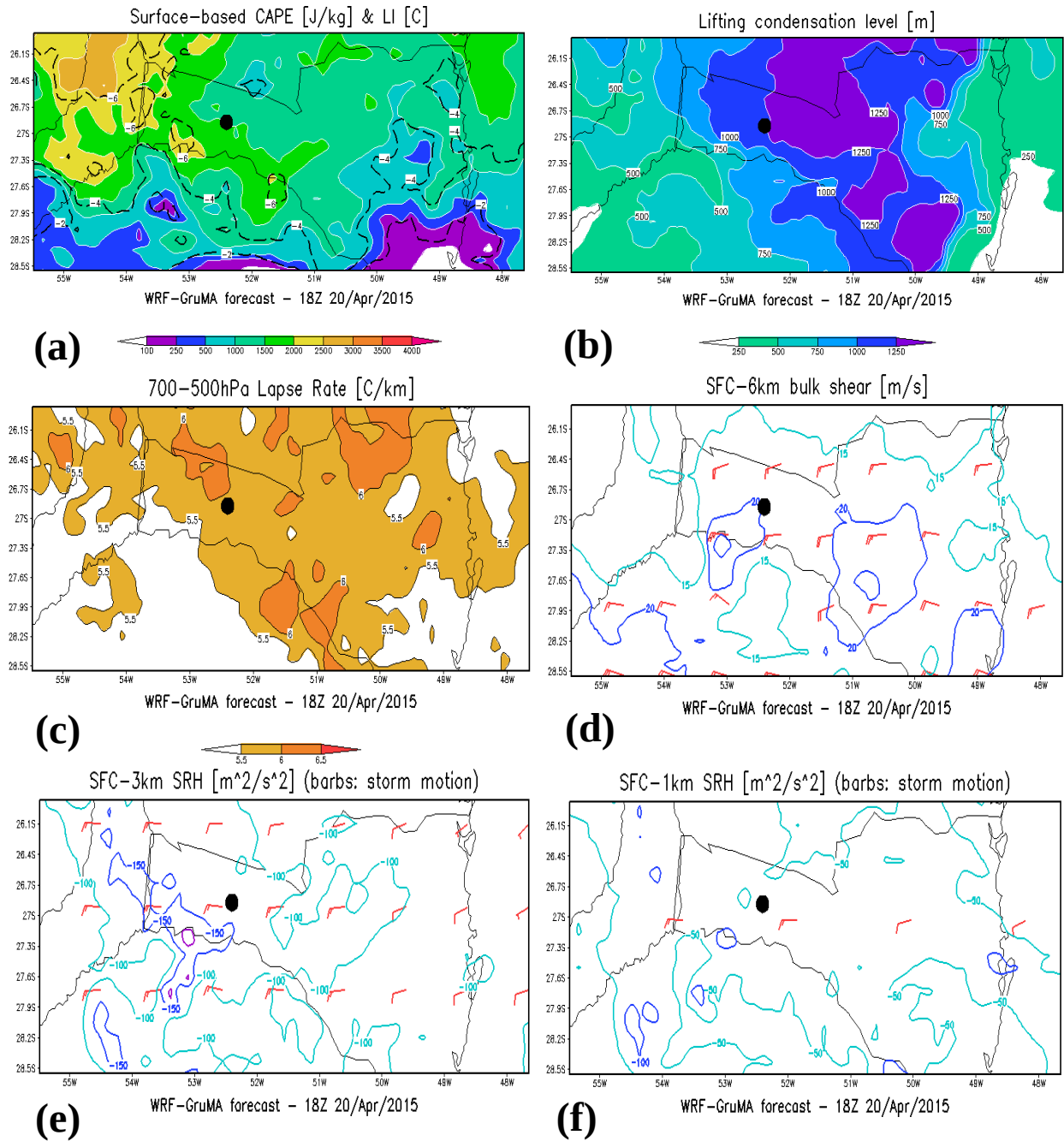


Figure 5: ARW-WRF 12-km 18-hour simulation valid at 18:00 UTC 20 April 2015, centered on SC. (a) CAPE (J kg^{-1}) and Lifted Index (contoured at $-1\text{ }^{\circ}\text{C}$ intervals) for a surface-based air parcel. (b) LCL height (shaded at 250 m intervals). (c) 700-500-hPa Lapse Rate (at 0.5 K km^{-1} intervals); (d) 0-6 km shear (contoured at 5 m s^{-1} intervals); (e) 0-3 km SRH (contoured at $-50\text{ m}^2\text{ s}^{-2}$ intervals); (f) 0-1 km SRH (contoured at $-50\text{ m}^2\text{ s}^{-2}$ intervals). The black dot in the figures denotes the location of Xanxere/SC.